arXiv:nucl-th/9606028v1 14 Jun 1996

LBL–38619
UC–413

Dilepton Production at SPS-Energy Heavy Ion Collisions[1][2]

Volker Koch and Chungsik Song

Nuclear Science Division, Lawrence Berkeley National Laboratory,
University of California,
Berkeley, CA, 94720, U.S.A.

Abstract

The production of dileptons is studied within a hadronic transport model. We investigate the sensitivity of the dilepton spectra to the initial configuration of the hadronic phase in a ultrarelativistic heavy ion collision. Possible in medium correction due to the modifications of pions and the pion form factor in a hadronic gas are discussed.

[1]Dedicated to Gerry Brown in honor of the 32^{nd} celebration of his 39^{th} birthday.

[2]This work was supported by the Director, Office of Energy Research, Office of High Energy and Nuclear Physics, Division of Nuclear Physics, Division of Nuclear Sciences, of the U.S. Department of Energy under Contract No. DE-AC03-76SF00098.

1 Introduction

One of the major goals of the ultrarelativstic heavy ion program is to study the restoration of chiral symmetry at high temperatures and densities and possibly to create and identify a new form of matter the so called Quark Gluon Plasma. To this end the measurement of electromagnetic probes such as photons and dileptons have continually attracted great interest. Contrary to hadronic observables these weakly interacting probes are not affected by final state interactions and thus may provide information about the early, hot stage of the reaction. While at very high invariant masses, above that of the J/Ψ the dilepton yield is essentially dominated by the Drell-Yan production from the hard nucleon nucleon collisions, it has been suggested that in the mass region between the Φ and the J/Ψ, dileptons originating from the QGP can be observed (for an overview see e.g. ref. [1]). Of particular interest in the high invariant mass region has been the study of the suppression of the J/Ψ, because of its possible implications about deconfinement. At low invariant masses, below 1 GeV the dilepton spectrum is expected to be dominated by the hadronic phase, where processes such as hadronic decays and pion annihilation contribute. This region is of particular interest, because possible in medium modifications of hadron masses such as that of vector mesons may be observable in the dilepton invariant mass spectrum [2, 3, 7]. This mass region is also accessible at lower bombarding energies (BEVALAC, SIS) where modifications of hadron masses due to finite nuclear density rather than temperature can be studied [8, 3]

Recently interest [11, 12, 22, 5, 13, 14] in the low mass region has been sparked by the experimental data from the CERES collaboration [9], which show a considerable enhancement at invariant masses of about 400 MeV for SPS-energy S+Au heavy ion collisions as compared to proton-proton as well as proton-nucleus collisions. A similar enhancement has also been seen by the HELIOS collaboration at more forward rapidities [10]. It has been suggested [11, 12] that this enhancement may be due to the dropping of the vector meson masses at finite temperature and densities, as proposed in [15, 16]. However, also more conservative effects, such as a modified in medium pion dispersion relation may give sufficient enhancement [5, 22]. This later effect has first been suggested in the context of BEVALAC energy heavy ion collisions [17, 18, 19] where the pion dispersion relation is modified due to the interactions with nucleons forming deltas. At SPS energies, one would expect that the major modification should come from interactions among pions, mostly in the the isovector - p-wave channel, which is dominated by the s-channel rho-meson resonance [20, 21]. The effect of the nucleons, however, may not be negligible [22].

However, before definite conclusions about possible in medium effects of any kind can be drawn, a conventional explanation of the observed enhancement has to be ruled out. The cocktail used by the CERES collaboration to estimate the conventional background includes only the decay of hadrons with a relative abundance taken from proton proton

data and scaled with the number of charged particles. In a heavy ion collision several things could be different from these assumptions due to multiple elastic and inelastic scatterings. First of all the relative abundance could be altered due to creation an destruction of higher lying meson resonances such the ρ or the a_1. Secondly, there could be multiple π-π annihilation processes leading to additional dilepton yields. Furthermore, initially , after formation, the hadrons not necessarily have to be in thermal equilibrium. One rather could imagine that a great deal of the thermalization observed in the final (freeze out) state [23] actually takes place within the hadronic phase. This equilibration, which involves elastic and inelastic collisions, then may result in a quite different dilepton yield as, for instance, obtained from an equilibrated hadron gas. In other words, a careful and systematic investigation of the dilepton production may reveal information about the equilibration properties of the hadronic phase.

It appears rather unlikely, on the other hand, that the equilibration process can be inferred from hadronic observables only. Provided that a certain degree of equilibration has been obtained in the final state, as suggested by a recent analysis of AGS as well as SPS data [24, 23], it is of course impossible to extract in which way the system has reached this point. Penetrating probes, however, are not only sensitive to the final state but represent an integral over the entire reaction history and thus are much better suited to constrain our understanding of equilibration dynamics. In other words, the fact the event generators such as RQMD [25] or VENUS [26] are able to reproduce most hadronic observables not necessarily implies that they simulate the reaction dynamics properly, since there are infinitely many trajectories towards thermal equilibrium.

The purpose of this article is to investigate the sensitivity of the dilepton yield to different initial conditions in the hadronic phase and to see to which extent the CERES and HELIOS data can be accounted for by non equilibrium processes in the hadronic phase. Our strategy therefore is to parameterize the initial phase space and the abundances of the hadrons subject to the constraint, that the final hadronic spectra and rapidity distributions are reproduced. This will lead to a set of initial conditions for which we then study the contribution to the dilepton data.

This paper is organized as follows: In the first section we will describe the hadronic transport model. In the second section we will describe the initialization of the hadronic phase space. In the third section the production of dileptons within out transport model will explained. We then will turn to the discussion of possible medium effect before we present the results and our prediction for Pb+Pb collisions.

2 Transport Model

In this section we will describe the hadronic transport model used to study the dilepton production. In our calculation we include pions, ρ- ω- and a_1 mesons as well as nucleons and deltas for the baryons. We ignore higher baryon resonances at this time but we will present an estimate of their contribution to the dilepton spectrum below. Since the fraction of baryons in the relevant rapidity region is small compared to that of the pions, we do not expect that they contribute significantly to the equilibration process. We have also left out the strange mesons for the same reason. The contribution of the eta meson to the dilepton yield is calculated at the end using the measured eta/pi ratio [27].

The interaction between nucleons, deltas and pions is done in the standard fashion as reported e.g. in [28, 29, 30] and we refer the reader to these references for details.

All hadronic resonances are propagated explicitly. For instance the resonant isovector p-wave $\pi - \pi$ scattering in the ρ channel is split into the formation, the propagation and the decay of a ρ-meson. As a consequence the mass of these resonances are not restricted to their central value but may assume any value as determined by the production process of by the initialization procedure (see below). To be specific, for the formation of the ρ from $\pi - \pi$ collisions, we use an isospin averaged Breit-Wigner cross section

$$\sigma_{\pi\pi\to\rho}(M) = \frac{8\pi}{p^2}\frac{\Gamma_\rho^2(M)M^2}{(m^2 - m_\rho^2)^2 + M^2\Gamma_\rho^2(M)} \tag{1}$$

Here p is the center of mass momentum and M the invariant mass of the pair. Using the standard π-ρ coupling [31] the width of the ρ is given by

$$\Gamma_{\rho\to\pi\pi}(M) = \Gamma_{0,\rho}\frac{p^3}{p_0^3}\frac{m_\rho^2}{M^2} \tag{2}$$

where p is the decay momentum. $\Gamma_{0,\rho} = 150\,\mathrm{MeV}$ and p_0 are the width and the decay momentum at peak value ($M = m_\rho$).

The formation and decay of the a_1 is a little more complicated since it involves a hadronic resonance, the ρ, in the initial or final state, respectively. Thus, the a_1 does not necessarily decay into a ρ of mass $m_\rho = 770\,\mathrm{MeV}$ but also into states with smaller and larger masses. As a starting point, we use the formula of reference [32] for the decay width of the a_1 into pion and ρ

$$\Gamma_{a_1}(M, m_\rho) = \frac{G_{a_1\rho\pi}^2 p}{24\pi m_{a_1}^2}\left(\frac{1}{2}(M^2 - m_\rho^2 - m_\pi^2)^2 + m_\rho^2(m_\pi^2 + p^2)\right) \tag{3}$$

Notice, that in the above formula the width depends also on the mass of the outgoing ρ. Therefore, if we want to allow for the decay into ρ-mesons with masses different from the

central value the total a_1-width should be given by the integral of the above formula over all kinematically allowed ρ-masses weighted with the ρ mass distribution $f_\rho(m)$. Hence

$$\Gamma^{tot}_{a_1}(M) = \int_{2m_\pi}^{\infty} f_\rho(m_\rho)\Gamma_{a_1}(M, m_\rho) \tag{4}$$

with

$$f_\rho(m) = \frac{2}{\pi}\frac{m^2\Gamma_\rho(m)}{(m^2 - m_\rho^2)^2 + m^2\Gamma_\rho^2} \tag{5}$$

We thus have to adjust the coupling G in eq. (3) such that the total width $\Gamma^{tot}_{a_1}$ agrees with the experimental value of 400 MeV. We find $G_{a_1\rho\pi} = 18.1\,\mathrm{GeV}^{-2}$. The *partial* width for the decay into a ρ of a specific mass is then given by

$$\frac{d\Gamma}{dm_\rho} = f_\rho(m_\rho)\Gamma_{a_1}(M, m_\rho) \tag{6}$$

This then gives the distribution from which the mass of the outgoing ρ has to be picked. Finally, the isospin averaged cross section for the formation of an a_1 in a $\pi - \rho$ collision is given by

$$\sigma_{\pi\rho\to a_1}(M) = \frac{3\pi}{4p^2}\frac{M^2\,\Gamma_{a_1}(M, m_\rho)\Gamma^{tot}_{a_1}(M)}{(M^2 - m_{a_1}^2)^2 + M^2\Gamma^{tot\,2}_{a_1}(M)} \tag{7}$$

where $\Gamma_{a_1}(M, m_\rho)$ is given by eq. (3) and $\Gamma^{tot}_{a_1}(M)$ is given by eq. (5). The advantage of this somewhat complicated prescription is that it allows to include the finite width of the ρ and, at the same time, preserves detailed balance.

For the ω meson we adopt a similar strategy. We model the dominant decay into three pions as a two step process via an intermediate $\pi\,\rho$ state, as suggested by chiral models including vector mesons [33]. Thus in our approach the ω decays into a pion and a ρ-meson the mass of which is below the central value. As explained previously in our transport model these ρ's are treated as real particles. To preserve detailed balance we also allow for the formation of the ω by $\pi\,\rho$-fusion.

Following ref [33] we use a p-wave form for the decay width of the ω

$$\Gamma_\omega(m_\rho) = Cq^3 \tag{8}$$

where q is the decay-momentum of the omega in its rest frame. The constant of proportionality, C, is then determined such that the total width, integrated of all possible ρ - masses with the proper weighting, corresponds to the observed experimental value for the decay into three pions

$$\Gamma^{tot}_\omega = C\int_{2m_\pi}^{m_\omega - m_\pi} f_\rho(m_\rho)\,q^3\,dm_\rho = 7.4\,\mathrm{MeV} \tag{9}$$

which gives a value of $C = 48\,\mathrm{GeV}^{-2}$.

Following the same arguments as in case of the a_1 the isospin averaged cross section for the formation of the ω is then given by

$$\sigma(M, m_\rho) = \frac{4\pi}{9q^2} \frac{\Gamma_\omega(m_\rho)\,\Gamma_\omega^{tot}}{(M^2 - m_\omega^2) + M^2\Gamma_\omega^{tot\,2}} \tag{10}$$

Naturally, due to the small width of the ω very few new ω are being formed in the course of the expanding hadronic system. Therefore, the resulting dilepton spectrum is only slightly changed as compared to calculations which do not take the formation of the omega into account [11].

Finally, for the non resonant scatterings we assume a constant cross section of 20 mb except for that among nucleons and Deltas, where a parameterization of the measured nucleon-nucleon cross section is being used.

3 Initialization of initial Phase space

As already outlined in the introduction, in our transport model we will not describe the entire collision history, starting from the initial colliding nuclei. We rather want to ask the question about the sensitivity of the dilepton production to the hadronic phase-space configuration created in such a collision. Thus the initial stage in our description is that of a hadronic gas with a possible non equilibrium configuration in momentum space. We also do not impose chemical equilibration. We, however, require that measured hadronic spectra and rapidity distributions are reproduced at the end of the evolution. As we shall see this leaves quite a number of possibilities to initialize the system.

3.1 Configuration Space:

We will assume that initially all particles are distributed uniformly within a cylinder of radius R_0 and longitudinal extent $2Z_l$. This somewhat simplified prescription may be improved by e.g. using a Gaussian distribution in the longitudinal direction, which we do not consider here. However, we should point out that the introduction of a formation time, discussed below, will effectively introduce some smearing of the particle density in the longitudinal direction. Since we plan to compare with the CERES data for $S + Au$ collisions, we will assume an initial transverse radius of $R_0 = 3.5\,\mathrm{fm}$. The longitudinal extent will be varied and the specific choices will be given in the results section (6).

3.2 Momentum Space:

Momenta in the transverse direction are distributed according to a two dimensional Bose- or Fermi- distribution with the possibility of non vanishing chemical potential. The chemical potential of the ρ is then twice that of the pion and those of the ω and a_1 three times the pionic one.

For the longitudinal momenta we assume that the rapidities of the particles are distributed according to a Gaussian distribution,

$$f(y,z) = \frac{1}{\sqrt{2\pi\sigma^2}} \exp\left[\frac{-(y - \frac{Y_l}{Z_l} z)}{2\sigma^2}\right] \tag{11}$$

which allows to take into account possible correlations between rapidity and longitudinal position z. To some extent, correlations between the longitudinal position and the rapidity are already generated by the introduction of a formation time as we will discuss below.

For the hadronic resonances the initial distribution of the masses has to be specified as well. In principle there are two possibilities. First, the masses are distributed according to the respective Breit Wigner distribution $f_{hadron}(m)$. Second, assuming that thermal equilibration has been achieved prior to hadronization, the masses should be distributed according to thermally weighted distribution, which slightly favors lower mass states. Assuming boost invariance on gets

$$f_{thermal}(m) = \frac{1}{N} f_{hadron}(m)\, m^2 T K_2(m/T) \tag{12}$$

where T is the transverse temperature, K_2 is the modified Bessel-function, and N is a normalization factor. Notice, that one obtains the same mass distribution in case of a Bjorken type fire cylinder. In this work we will only consider the second possibility (12).

3.3 Formation Time:

A realistic description of the initial hadronic fireball should include a formation time. Particles with higher rapidities will be created at later times in a given frame of reference. In our approach we assume that particles will propagate *without* interaction for times smaller than their formation time

$$t_{formation} = \tau \cosh(y) \tag{13}$$

where y is the rapidity of the particle under consideration and τ denotes the proper formation time. This formation time clearly introduces a smearing of the longitudinal distribution in configuration space in the sense that, at the time particles will be allowed to interact, the fastest ones have already moved a considerable distance $\delta z \simeq t_{formation}\, c$. For the same reason the formation time leads to a rapidity longitudinal-position correlation.

3.4 Particle Abundances:

In order to reproduce the measured rapidity spectrum of protons by the NA35 collaboration [34] we assume that our hadronic fireball contains 60 baryons. The relative weighting is then determined by the temperature assuming thermal and chemical equilibrium. At the temperatures considered here we will have about as many nucleon as deltas.

For the mesons we will either use the relative abundances as determined from proton proton collisions, i.e $N_\rho/N_\pi = 0.2$, $N_\omega/N_\rho = 1/3$. Since the number of a_1 is not given by experiment we assume $N_{a_1}/N_\omega = 0.5$.

Alternatively, we will assume initial chemical equilibrium and will determine the relative abundances assuming a boost invariant momentum distribution. In this case the abundances of course depend on the initial temperature and will therefore be given in the appropriate context in the results section (6).

3.5 Flow:

Several analyses of available SPS data suggest that there is substantial radial flow, which leads to larger apparent temperatures [35, 23]. We, therefore, allow for the possibility that the hadrons have some transverse flow in the initial state. For simplicity we assume a constant flow velocity independent of the radial distance of the particle. To generate the flow, we first distribute the particles thermally in the transverse direction, then we boost them according with the flow velocity before we finally boost them in the longitudinal direction as given by the initial rapidity distribution. This sequence of boost is identical to that employed by Schnedermann et al. [35]. Allowing for transverse flow reduces the initial temperature needed to reproduce the final transverse momentum spectra. We should point out, however, that in our transport model a certain amount of flow is generated as result of particle collisions. Therefore, the initial flow velocities used here should not be compared directly with results from the analysis of hadronic spectra.

4 Dilepton production

Having specified the initial phase space distribution as well as transport model we finally turn to the production of dileptons. As far as dilepton production through pion annihilation is concerned there are essentially two ways to proceed in a transport model, which are in principal equivalent. One is to directly calculate the dilepton yield from the pion collisions and the other one is to obtain the dileptons from the decay of the ρ which has been formed in the collisions. Both are equivalent as has been shown in [7, 11]. However, we found that the second prescription is extremely sensitive to statistical fluctuations for invariant masses smaller that 400 MeV, as we will explain below. We, thus, resort to the

first prescription, namely the production of dilepton directly from the $\pi\,\pi$ collisions. We use the well known cross section

$$\sigma_{\pi+\pi\to e^+e^-}(M) = \frac{2}{9}\frac{4\pi}{3}\frac{\alpha}{M^2}\sqrt{1-\frac{4m_\pi}{M^2}}\frac{m_\rho^4}{(M^2-m_\rho^4)^2+M^2\Gamma_\rho(M)^2} \tag{14}$$

where the factor $\frac{2}{9}$ arises from isospin averaging.

All the Dalitz decays are done explicitly. Therefore, in order to avoid double counting, only the ρ mesons present in the initial state are allowed to decay into dileptons. All secondary ρ mesons come from processes such as pion annihilation or a_1 decay, where we take the contribution to the dilepton yield into account explicitly, including vector dominance, so that those ρ mesons should not decay into dileptons.

We furthermore include the direct decay of the ω into dileptons as well as the Dalitz-decay of the η meson. As already pointed out previously, we do not explicitly propagate the η, but include it at the end of the calculation. To that end we assume that the etas have the same rapidity distribution as the pions. The relative abundance and the transverse momentum spectrum we obtain from the measured η/π_0 ratios as a function of p_t provided by the WA80 collaboration [27].

In order to improve statistics we treat the dilepton decay 'perturbatively', i.e. at each time step the particles are allow to 'radiate' dileptons, without being removed. The contribution to the final spectrum is then given by the partial width multiplied by the time step size $\Gamma_{e^+e^-}\,dt$. At the end of the calculation all remaining hadrons are forced to decay and their contribution to the dilepton spectrum is given by the respective branching ratios. In case of the pion annihilation, any $\pi\,\pi$ collision contributes to the dilepton yield with the ratio of dilepton production cross section over total cross section.

For a comparison with the CERES data, cuts on the lepton momenta have to be performed. In order to improve our statistics further we sample the decay of each virtual photon several (ten) times.

For the Dalitz decays of the η and ω we use the formulae of Landsberg [36] including form factors. For the form factors we use the values given in [36]

$$f_\eta(m) = (1-2.4\,m^2)^2 \tag{15}$$
$$f_\omega(m) = (1.-m^2/0.72^2)^2 \tag{16}$$

where the invariant mass m is to be given in GeV.

For the a_1 we also use the Landsberg formula with a vector dominance form factor including the width of the ρ

$$f_\rho(m) = \frac{m_\rho^4}{(M^2-m_\rho^4)^2+M^2\Gamma_\rho(M)^2} \tag{17}$$

We have compared this formula with an explicit calculation of the Dalitz decay of the a_1 using the Lagrangian of [32] an found very good agreement.

For the partial decay width of the ρ we use [31]

$$\Gamma_{\rho_0 -> e^+e^-}(M) = \Gamma_0 \frac{m_\rho^3}{M^3} \tag{18}$$

where $\Gamma_0 = 6.77\,\mathrm{keV}$ is the measured width at peak value. Notice, that for small invariant masses the branching ratio for a ρ decaying into dileptons increases rapidly since the total width, which is dominated by the p-wave decay into pion becomes small. As a consequence if an initial ρ with small invariant mass happens to survive until the end of the calculation it will decay with a very large branching ratio. We find that for 400 runs the average number of ρ with small invariant masses surviving until the end (30 fm/c) is less than one and thus the statistical fluctuations are tremendous. By changing the random number seed the results for invariant masses smaller that 400 MeV fluctuated by more than an order of magnitude. Since this mass region is identical to the one where the CERES collaboration reports a strong enhancement, these uncertainties are unacceptable. We should also point out that we have observed similar fluctuations when we calculated the pion annihilation in a two step process, i.e. via the formation and the decay of the ρ meson. To avoid those we resorted to the direct production of dilepton from pion collisions as described above. In order to circumvent the statistical fluctuations from the ρ mesons in the initial state we calculate the contribution to the dilepton spectrum from ρ mesons with masses smaller than 500 MeV directly, i.e. not by Monte Carlo methods. To this end we calculate the number $N_\rho(M)$ of ρ meson in a given mass interval $M + \Delta M$ from the mass and phase space distribution. The dilepton yield is then obtained by multiplying with the branching ratio

$$\frac{dN_{e^+e^-}}{dM} = N_\rho(M) \frac{\Gamma_{\rho \to e^+e^-}}{\Gamma_{tot}} \tag{19}$$

Since $N_\rho(M)$ is proportional to Γ_{tot} the above distribution is smooth even if Γ_{tot} becomes small. By calculating the decay of these small mass ρ mesons directly we ignore possible absorption effects and thus somewhat overestimate the yield at low invariant masses. Naturally, in order not to double count, all initial ρ mesons with masses below 500 MeV are not allowed to decay in dileptons during the expansion.

5 Medium modifications

One of the most interesting aspects of studying low mass dilepton pairs is the possibility to learn something about in medium modifications of hadrons. One possibility is to see

the possible dropping of the mass of vector mesons [2, 7] as proposed by Pisarski [15] as well as Brown and Rho [16]. In the context of the CERES data, this possibility has been studied in references [11] as well as [12]. However, as far as the restoration of chiral symmetry is concerned, the dropping of the vector meson masses are at best an indirect signature. To leading order in the temperature chiral symmetry predicts no change in the mass of the vector mesons [37]. This finding is also confirmed by calculations using effective chiral Lagrangians [38, 39].

In this article we want to concentrate on two medium effect which have been discussed in detail in ref [4, 5, 6], namely the reduction of the pion form factor due to the onset of chiral restoration and the effect of the in medium pion dispersion relation. As demonstrated in ref. [5] both effects combine to flatten the invariant mass distribution of dileptons in qualitative agreement with the CERES data. In ref. [5] the contributions of other production channels have not been taken into account. Also the effect of the experimental cuts have been ignored thus not allowing for a quantitative comparison with the data. Here we will attempt a first quantitative comparison with the data by including the above medium effects into our transport model. This is done in the following way: For each $\pi\pi$ collision we determine the local temperature from the local covariant pion density

$$\rho(x) = \int \frac{d^3p}{2\omega(p)(2\pi)^3} f(x,p) \tag{20}$$

where $f(x,p)$ is the pion phase space distribution. Assuming local thermal equilibrium we obtain the temperature from

$$T(r) = \sqrt{\frac{\rho(r)(2\pi)^2}{3}} \tag{21}$$

where $\rho(r)$ denotes the pion density at position r. Given the local temperature we multiply the pion annihilation cross section by the ratio between in medium and free production as determined in ref. [5, 6] (see fig 1).

This procedure involves several approximations: First, we ignore any non equilibrium effects on the in medium corrections. This, however, may not be such a bad approximation, since to leading order in the temperature the in medium corrections are really effects of the pion density, which we use to extract the temperature. Secondly, we do not propagate the pions according to their in medium dispersion relation, but only take its effect into account when determining the annihilation cross section as described above. This, however, leads only to a slight difference in the overall reaction dynamics as demonstrated in ref. [40]. Finally, our largest and so far least controlled approximation is to assume that the pion-form factor does not depend on its momentum with respect to the heat bath.

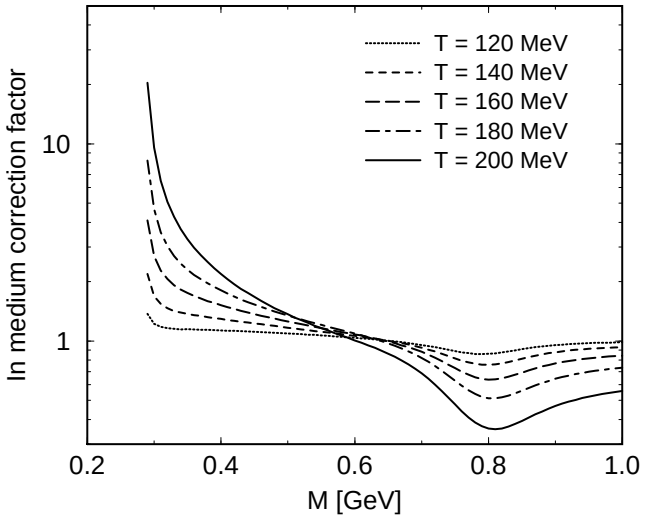


Figure 1: Correction factor used in in medium calculation for the pion annihilation cross section

The determination of the momentum dependence represents a rather involved computation which we are currently trying to work out. However, considering the comparatively small contribution from the pion-pion annihilation (see below), we do not expect that the correction from the true momentum dependent form factor will alter our conclusions substantially.

6 Results and Discussion

Before we discuss our result in detail let us summarize our findings. By playing with the initial conditions for the hadronic system we could generate variations in the dilepton spectra, subject to the CERES acceptance cuts by at best a factor of two. A large portion of these variations arises from the contribution of the eta - Dalitz decay, and, therefore, is due to a principally measurable quantity. Considering the the large systematic and statistical errors of the present CERES data, we unfortunately cannot conclude that these present data put strong additional constraints on the hadronic equilibration dynamics. With some initial conditions (not including medium modifications) we are able to come within the lower end of the sum of statistical and systematic error of the CERES data and at the same time obtain a reasonable agreement with the HELIOS data. We furthermore find that the in medium modification considered give only an insignificant enhancement

of the total dilepton yield. The reason for that is that the pion annihilation, although important, contributes at best a third of the total yield in the relevant low mass region. Therefore a factor of two enhancement reduces to less than 30 % enhancement in the total dilepton spectrum.

6.1 Dilptons from different inital states

Let us now turn to the detailed discussion of our results. We have investigated many different initial conditions and the most representative of those are listed in table (1). Following the discussion in section 3 the characterization of the initial hadronic system can be divided into two major groups

1. Momentum and configuration space (phase space). This includes choices for the formation time and possible initial radial flow.

2. Relative abundances of particles

The initial momentum space distribution is controled by the choice of rapidty distribution, transverse momentum distribution, initial flow velocity and, at least for the pions, a possible chemical potential. The only parameter we used to change the initial configuration space is the longitudinal extend of the fireball, assume that initially transverse motion is small. Finally, we can generate possible configuration space and momentum space correlations by either chosing a finite formation time or, explicitly, by a finite value of Y_l in eq. (11).

We find that an initial number of about 600 pions (possibly 'hidden' in ρ etc mesons) is needed. The relative abundances are either taken as those found in nucleon-nucleon experiments (indicated by '*pp*' in table (1)) or as given by chemical equilibrium (indicated by '*chem*' in table (1)). Whenever we have chosen chemical equilibrium abundances we also have assumed a vanishing formation time together with z-y correlations ($Y_l \neq 0$) and a slightly more extended fireball (typically $Z_l = 2\,\mathrm{fm}$, except sets 5 and 6)

In figures (3 – 8) we show the resulting dilepton invariant mass spectra using the parameter sets given in table (1). To demonstrate the typical agreement we tried to achieve with the pion spectra and the proton and pion rapidity distribution the initial and final distributions for parameter sets 1 and 2 are shown in fig. (2). For the p_t proton spectra the slope parameter of the final spectrum ($T_{final}(prot)$ is given in table (1). These should be compared with an experimental slope parameter of about $240MeV$ [42]. Since the protons only indirectly affect the dilepton production we did not put too much an effort in fine tuning the resulting proton spectra.

Parameter set 1 assumes that at the moment of hadronization the longitudinal position and the rapidity are correlated ($Y_l \neq 0$, see eq. (11)). This is similar to the initial

	Set 1	Set 2	Set 3	Set 4	Set 5	Set 6	Set 7	Set 8
ratios	p-p	p-p	p-p	therm	therm	therm	p-p	therm
N_π	350	350	350	114	156	270	1200	540
N_ρ	70	70	70	96	89	95	240	307
N_ω	24	24	24	60	62	31	80	214
N_{a_1}	12	12	12	36	25	15	40	86
τ [fm/c]	0	1	0.5	0	0	0	0.5	0
T_{init} [MeV]	240	200	200	260	190	160	160	190
μ_π [MeV]	0	0	0	130	130	0	0	130
Y_l	1.6	0	0	1.6	1.6	1.5	0	1.6
σ	0.55	1.5	1.5	0.55	0.6	0.7	1.8	0.6
Z_l [fm]	2	1.5	1.5	2	2.9	22	2.0	3.4
$Y_l(nucl)$	1.7	0	0	1.7	1.8	1.8	0	1.8
$\sigma(nucl)$	0.6	1.6	1.6	0.6	0.7	0.7	1.9	0.7
v_{flow}	0	0	0	0	0.35	0.4	0	0.4
T_{final}(prot.) [MeV]	235	230	250	240	260	250	250	290

Table 1: Parameter sets used for dilepton calculations for $S+Au$. The line labeled 'ratios' indicates whether the relative abundances are taken according to proton proton data (p-p) or according to thermal equilibrium (therm). The last row gives the slope parameter of the final proton spectrum.

conditions used by Li et al. [11]. The relative particle abundances are assumed to be the same as in proton proton collisions. This leads to about initial 350 pions. With the longitudinal extent of $R_l = 2Z_l = 4\,\mathrm{fm}$ and a radius of 3.5 fm the resulting initial pion density is then as large as $\rho_{init} = 2.3\,\mathrm{fm}^{-3}$, which is certainly larger then one would consider reasonable for a transport description[3]. The initial density is reduced if one uses thermal particle ratios, which, for the same longitudinal extend, corresponds to parameter set 4. There we have assumed a fairly large chemical potential of $\mu_\pi = 130\,\mathrm{MeV}$. In this case the pion density reduces to $\rho_{init} = 0.75\,\mathrm{fm}^{-3}$, which is an acceptable value for a transport description. Notice that the thermal pion density with that chemical potential and the temperature of $T_{init} = 260\,\mathrm{MeV}$ would be about twice as high. In this sense parameter set 4 also does not correspond to initial chemical and thermal equilibrium.

Initial densities consistent with the thermal ones are considered in parameter sets 5 and 6. Here we also have allowed for an initial transverse flow resulting in a lower initial temperature. The longitudinal extension of the fireball has then been fixed by requiring

[3]Notice, that due to the initial $z-y$ correlations the effective pion density is, however, somewhat lower

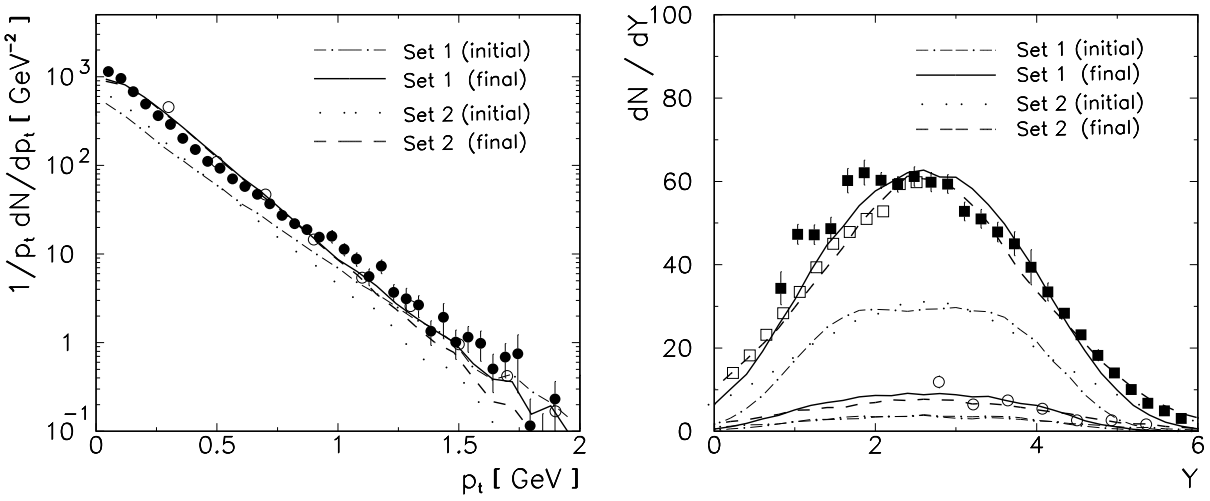


Figure 2: Pion transverse momentum spectrum (left) and pion and proton rapidity distribution (right) for parameter sets 1 and 2. The experimental data for the transverse momentum spectrum are from the NA35 collaboration [34] (full circles) and the WA80 collaboration [27] (open circles, errorbars left off). The data for the proton and pion rapidity distributions are from the NA35 collaboration [47]. The open squares are a reflection of the datapoints with $Y \geq 2.6$ with respect to $Y = 2.6$.

that the initial hadron densities agree with thermal values for the respective chemical potentials. In these cases the initial pion densities are lower, due to the smaller initial temperature. They are $\rho_{init} = 0.68\,\mathrm{fm}^{-3}$ and $\rho_{init} = 0.16\,\mathrm{fm}^{-3}$ for set 5 and 6, respectively

A complementary, and maybe more realistic picture of the initial hadronic state, is to assume that the creation of a hadron from string fragmentation requires a certain time, the so called formation time (see section 3). The introduction of a formation time considerably reduces the initial effective hadron density because only hadrons which have been formed are allowed to interact. These are essentially only the particles in the same rapidity interval. Parameter sets 2 and 3 have a formation time of $\tau = 1\,\mathrm{fm/c}$ and $\tau = 0.5\,\mathrm{fm/c}$, respectively. In this case we did not give the particles an initial $z - y$ correlation, since our physical picture is that particles are produced independently over the entire volume by the first hard nucleon-nucleon collisions. However, due to the finite formation time, for particles which are allowed to interact longitudinal position and rapidity are correlated. For the longitudinal extent we chose a size of $Z_l = 1.5\,\mathrm{fm}$, which corresponds to the Lorentz contracted longitudinal size of the combined sulfur and gold nuclei in the rest frame of the fireball. The initial temperature needed to reproduce the pion spectra is then $T_{init} = 200\,\mathrm{MeV}$.

Finally we should point out that in all parameter sets except sets 5 and 6 the relative width of the rapidity distributions (see eq. (11)) between π, ρ and ω has been taken from proton proton data [43]. These ratios are $\sigma_\rho/\sigma_\pi = \sigma_\omega/\sigma_\pi = 0.66$. For the a_1 we assume a slightly smaller ratio, namely $\sigma_{a_1}/\sigma_\pi = 0.5$.

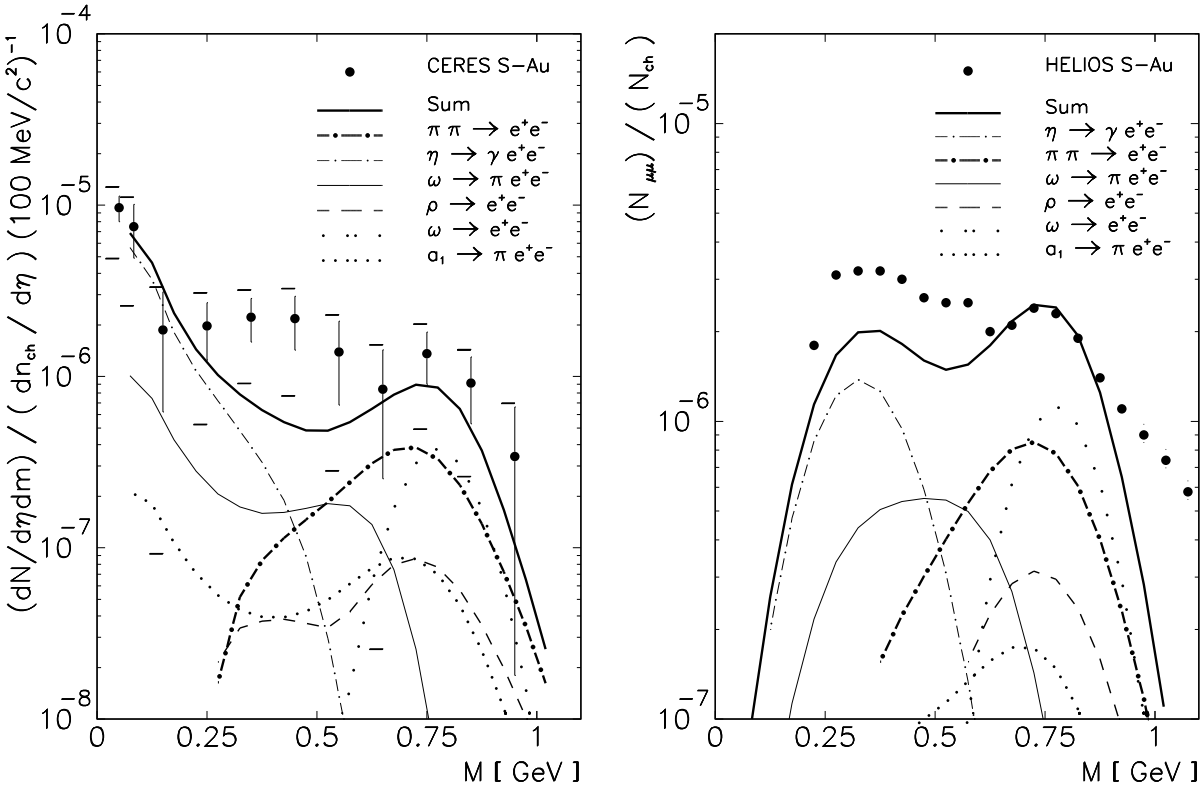


Figure 3: Dilepton production for parameter set 1

Parameter sets 1 and 2 (see figures 3 and 4) give essentially the same results for the CERES dilepton spectrum. The differences seen in the comparison with the HELIOS data around the ω mass demonstrates the effect of the formation time. In set 2, where we have a finite formation time of $\tau = 1\,\mathrm{fm}$ the contribution of the pion annihilation is reduced for the forward rapidities where the HELIOS acceptance is located.

The comparison with the calculations seems to suggest that the double hump structure in the HELIOS data is mainly due to η Dalitz decays at low masses[4] and the ρ / ω decays as well as pion annihilation at high masses. Consequently, possible small discrepancies at

[4]Notice, that HELIOS is measuring dimuons so that the minimum invariant mass is 200 MeV and, therefore, the rise in the η Dalitz spectrum does not appear as in the CERES spectrum.

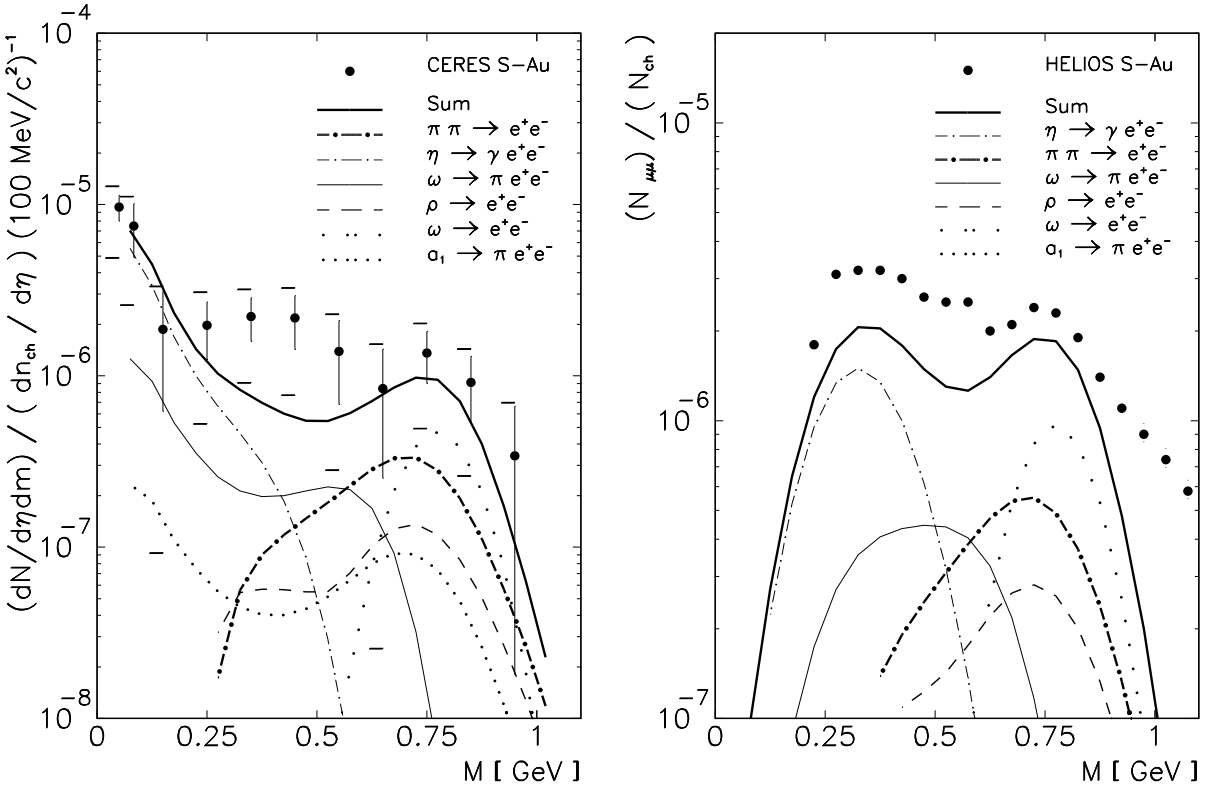


Figure 4: Dilepton production for parameter set 2

low invariant masses (at the 'η-hump') should only be taken seriously once a precise measurement of the η abundance at forward rapidities is available. Without this information the disagreements seen in our results can always be 'fixed' by fine tuning the forward pion rapidity distribution and the hard end of the pion transverse momentum spectrum, since we use m_t scaling to obtain the η mesons from the final pion distribution.

Reducing the formation time to $\tau = 0.5\,\mathrm{fm/c}$ (Set 3, figure 5) increases the contribution from the pion annihilation, bringing our results close to the lower end of the sum of statistical and systematic error bars of the CERES data in the interesting mass region around $400 - 500\,\mathrm{MeV}$. The agreement with the HELIOS data is pretty reasonable in this case except around an invariant mass of about 500 MeV, where we are about a factor of two too low, even if we fine tuned the η Dalitz contribution. In this case also the contribution of the η-Dalitz is slightly larger then in Set 1. Because of the shorter formation time more flow is generated which in turn gives a slightly harder pion spectrum (which, however, is still in very good agreement with the data) and thus a few (20 %) more η mesons.

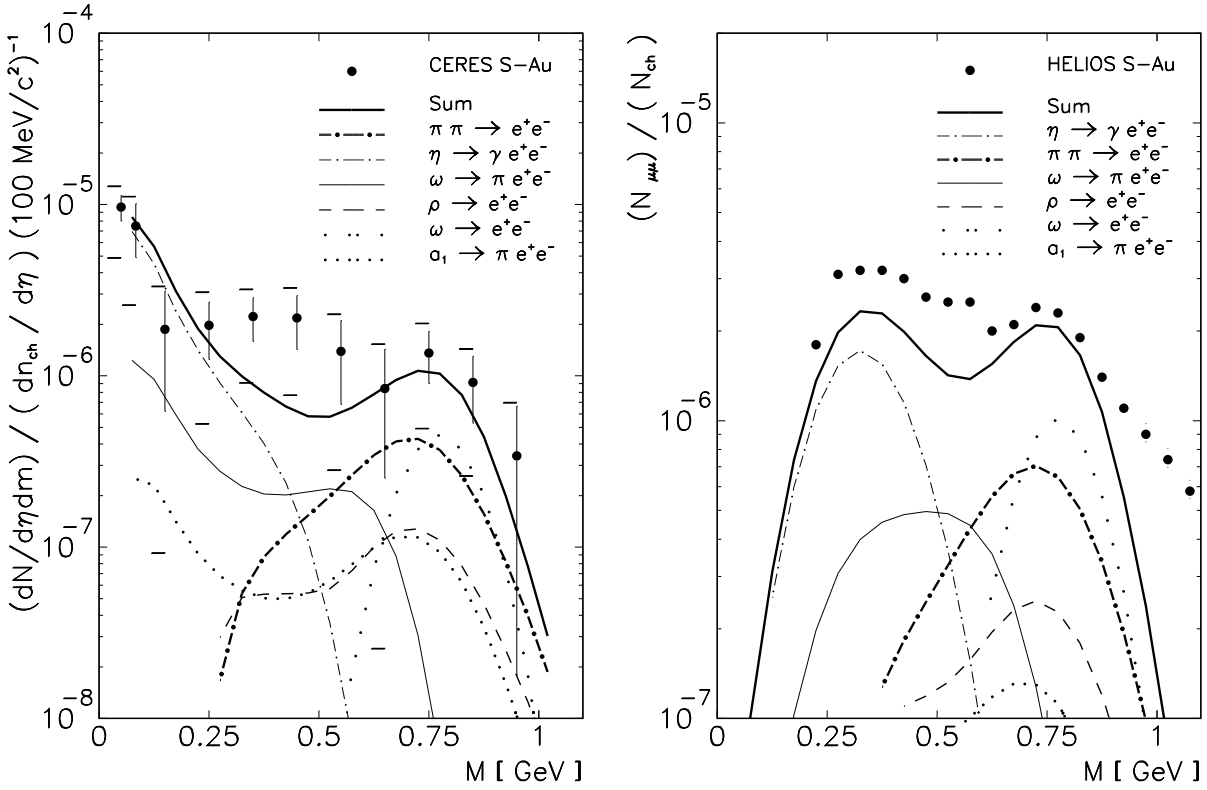


Figure 5: Dilepton production for parameter set 3

The one single process which contributes directly to the interesting region around $M \simeq 400 - 500\,\mathrm{MeV}$ is the Dalitz decay of the ω meson. Since the creation cross section of ω meson via π-ρ fusion is rather small the only way to increase the number of ω mesons is by assuming thermal particle ratios with a large pion chemical potential. This is done in parameter set 4, where we have assumed a pion chemical potential $\mu_\pi = 130\,\mathrm{MeV}$. Comparing with parameter set 1, this clearly increases the dilepton yield in the relevant mass region and the main contribution is from the ω-Dalitz decays. At the same time also the contribution of the direct decay of the ω is increased, leading to an overprediction of the HELIOS data in the ρ-ω mass region.

As already mentioned, for parameter sets 5 and 6 we have adjusted the longitudinal size of the fireball such that the particle density agrees with the thermal one. We have also allowed for initial radial flow and, as a result, the initial temperature is smaller. Furthermore, unlike in the previous cases, the widths of the rapidity distributions have been taken to be the same for all mesons. Assuming thermal densities, although apparently more consistent, reduces the hadron dynamics to some extent, in particular in case of set

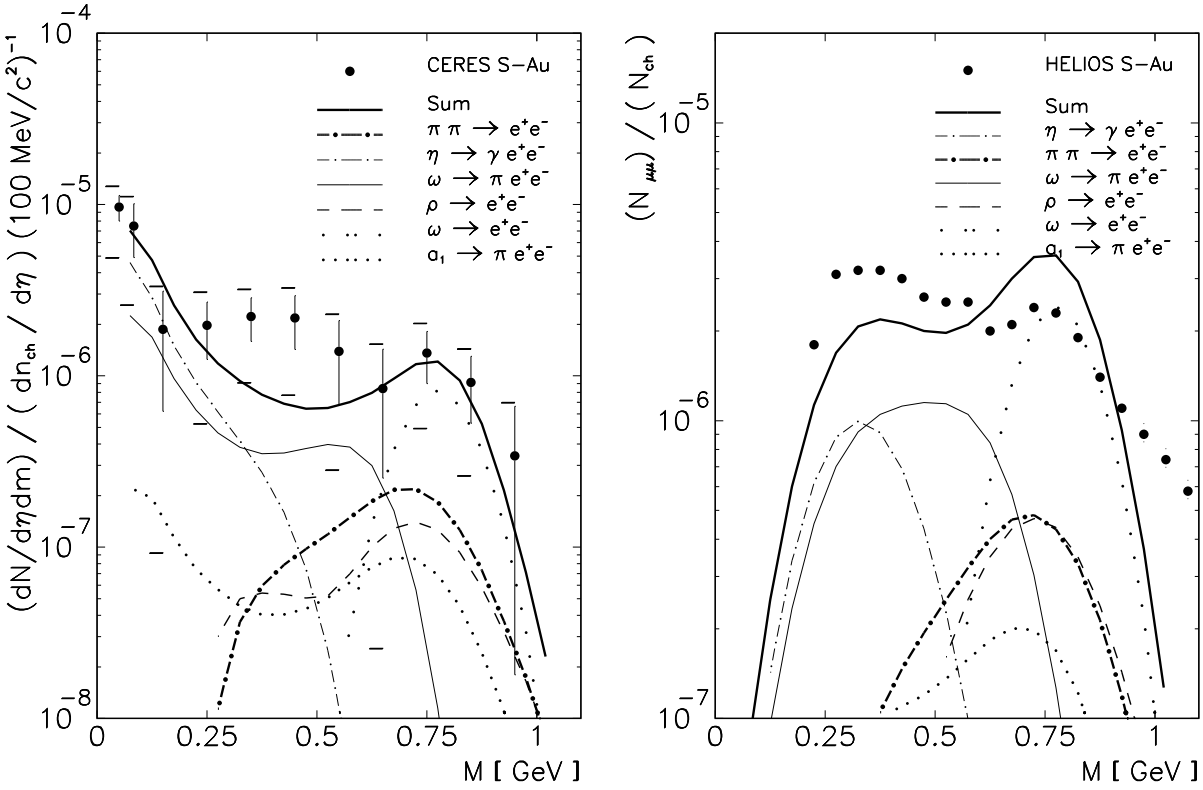


Figure 6: Dilepton production for parameter set 4

6, where we have a longitudinal size of 44 fm. These are essentially freeze out conditions and it appears rather unlikely that hadrons do not interact and/or have expanded in the radial direction before that. In case of set 5 the longitudinal extent is not much larger than in the comparable set 1 and this may be a more realistic scenario, where hadrons are created in thermal equilibrium. Again, because of the large pion chemical potential in set 5, there is a large fraction of initial omegas. Consequently, we find a sizeable contribution in the interesting mass region and an overshooting in the $\rho\,\omega$ region in case of the HELIOS data.

Additional information may be obtained by studying transverse momentum spectra of the dileptons once data of sufficient statistics are available. In figure 9 we show the resulting transverse momentum spectra using the parameter set 3 for the invariant mass regions $400\,\mathrm{MeV} \leq \mathrm{M} \leq 450\,\mathrm{MeV}$ (a) and $750\,\mathrm{MeV} \leq \mathrm{M} \leq 800\,\mathrm{MeV}$ (b), respectively. We do not observe any significant structure in the spectrum and all contributions look more or less exponential. Only in the ρ - ω mass range (b) the contribution of the omega decay shows a significantly larger slope parameter ('temperature'). This is essentially a result

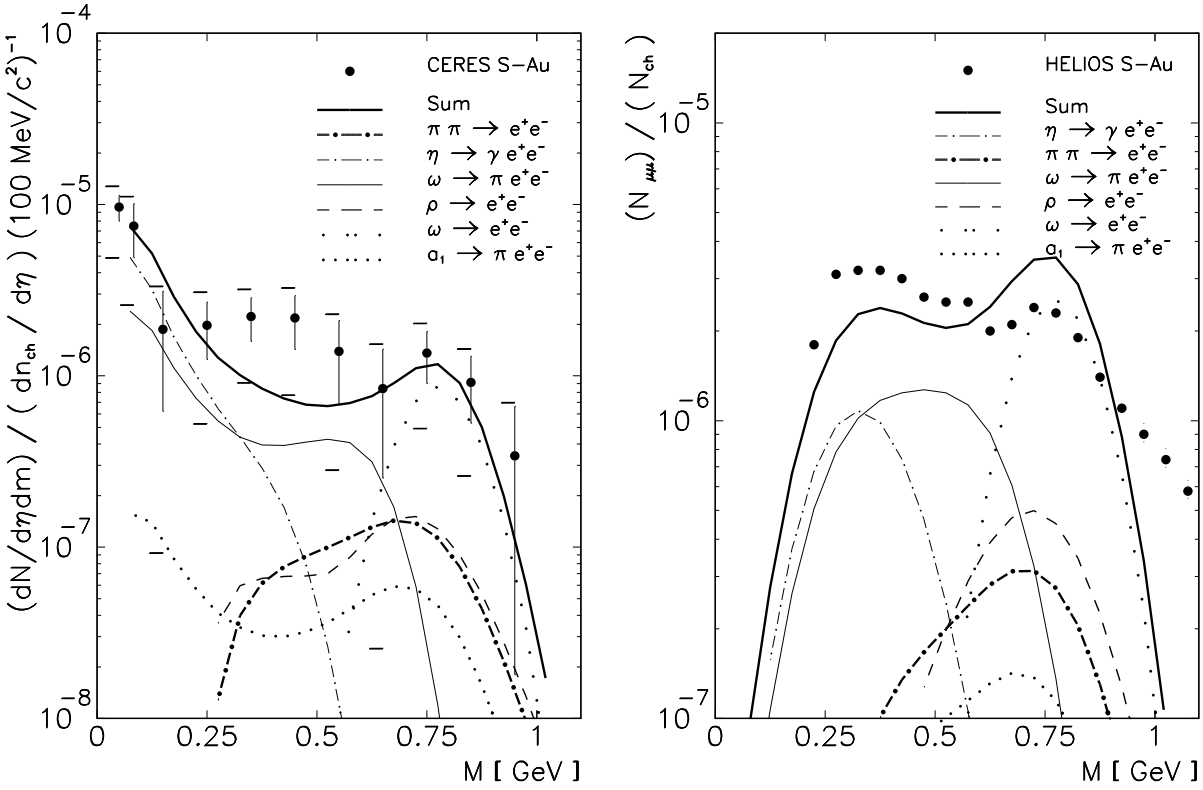


Figure 7: Dilepton production for parameter set 5

of the transverse flow which is generated during the expansion. This affects mostly the ω mesons, which decay predominantly after freeze out, i.e. after the transverse flow has been build up. Pion annihilation, the other strong contribution in this mass range, on the other hand, contributes mostly at the initial stage of the the expansion, and thus is not affected by flow. Therefore, already with the present mass resolution of the the CERES detector, the relative importance of the omega decays can be determined by a careful measurement of the slope parameter of the dilepton transverse momentum spectrum. This will then provide a crucial constraint to available model calculations.

To conclude this part, it appears that without any in medium effects we are able to more or less reproduce, within errors, the CERES data as well as the HELIOS data. Except for the first three data points, our 'best' result, set 3, seems to be consistent with the CERES data, if the points are shifted towards the lower end of the systematic error. Looking at the HELIOS and CERES data together, there seems to be some enhancement at an invariant mass slightly above 500 MeV. However, given the large systematic errors of the CERES data, and the fact that the systematic errors of the HELIOS data are

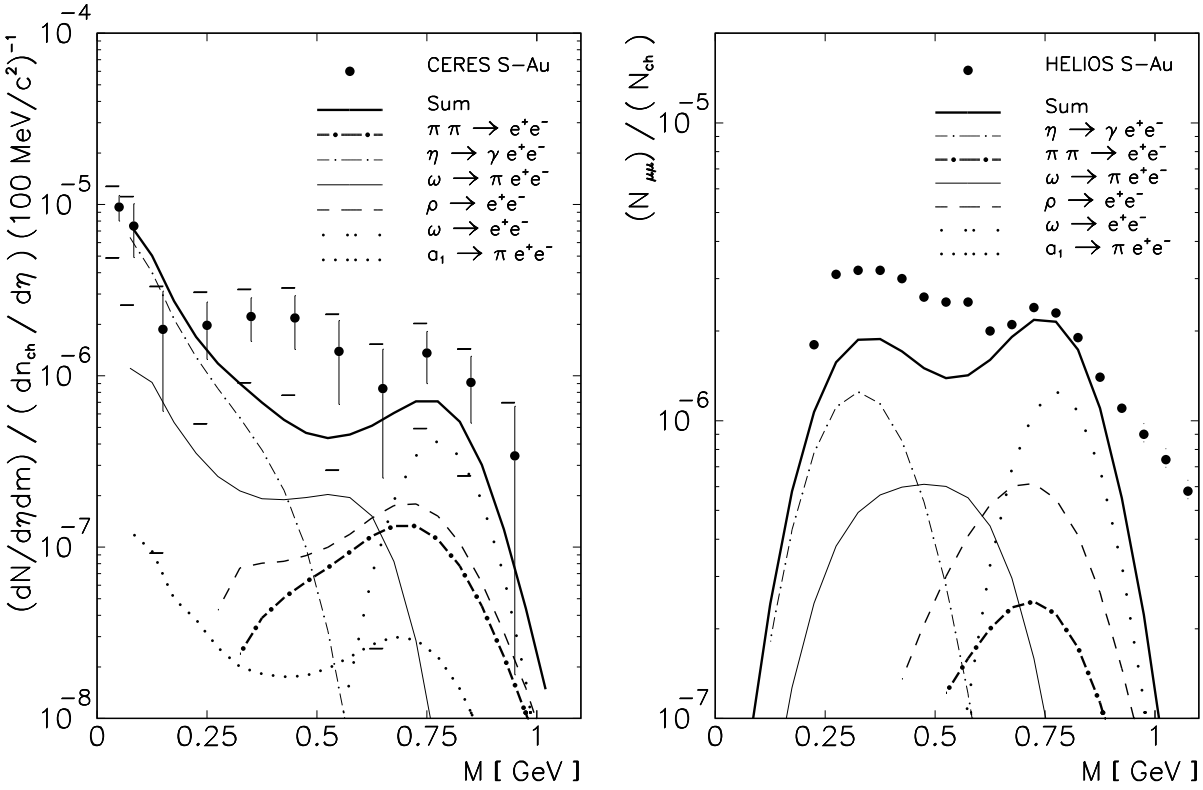


Figure 8: Dilepton production for parameter set 6

not given, it seems to be too early to declare the presence of any in medium effects. If, of course, an improved measurement would confirm the central values of the CERES data, from our investigations, we do not expect that any non-equilibrium effects of the hadronic phase would give that many dileptons in the relevant invariant mass region around $400 - 500\,\mathrm{MeV}$.

We have demonstrated that different initial hadronic configurations can lead to differences in the dilepton yield while still consistent with the hadronic observables. It also seems that the HELIOS data rule out initial partical ratios derived from chemical equilibrium based on a large pion chemical potential. Unlike the ρ, the decay of the ω into dileptons is not expected to be reduced as a result of the resoration of chiral symmetry [44]. Also, a possible collisional broadening of the omega would not change this, because the experimental resolution is already much larger than any expected in medium width of the omega [45].

From all the many configuration we have investigated (also those not reported here) it appears, however, that it is very unlikely to go above the lower end of the combined error

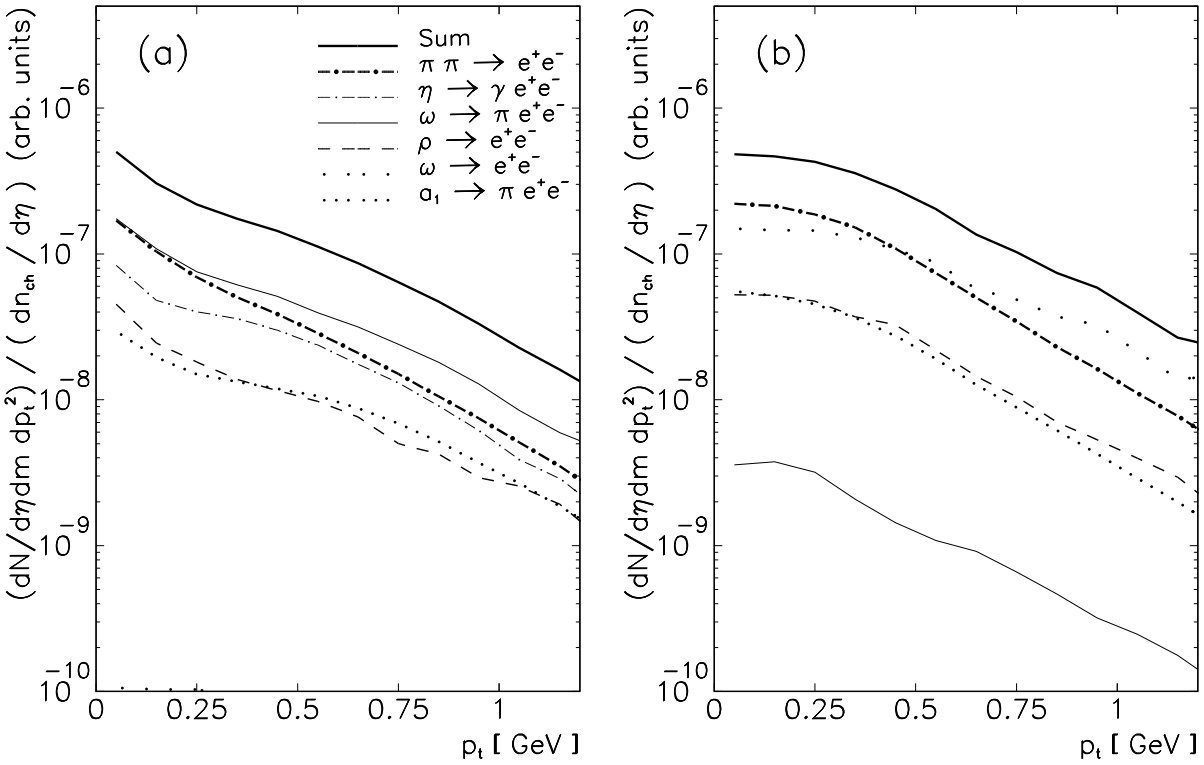


Figure 9: Transverse momentum spectra for dileptons using the CERES acceptance and parameter set 3. The ranges in invariant mass are $400\,\mathrm{MeV} \leq \mathrm{M} \leq 450\,\mathrm{MeV}$ (a) and $750\,\mathrm{MeV} \leq \mathrm{M} \leq 800\,\mathrm{MeV}$ (b)

of the CERES data the mass region around $400 - 500\,\mathrm{MeV}$. As we shall discuss in the following section, we also do not expect that our proposed in medium correction would improve the situation considerably.

6.2 Medium effects

Let us now turn to the results including the proposed in medium modification of the pion annihilation cross section (see section 5). Since our in medium modification only affects the pion annihilation let us consider the parameter set 3, which has the biggest contribution from this channel. This then gives an upper limit of what we should expect for the different scenarios considered here. The resulting dilepton spectra are shown in figure 10 together with the results without in medium effects, c.f. figure 5. We only show the total yield and the contribution from the pion annihilation. All other contributions

are identical to those in figure 5, since the way we implement the in medium corrections does not affect the expansion dynamics. While there is an enhancement in the pion annihilation contribution at low invariant masses and a suppression around the ρ-ω mass, the effect in the total spectrum is hardly visible, especially in the interesting mass region. This is simply due to the fact that the pion annihilation contributes less than 1/3 to the total yield in this region and even an enhancement of a factor of two would increase the total spectrum by less than 30 %.

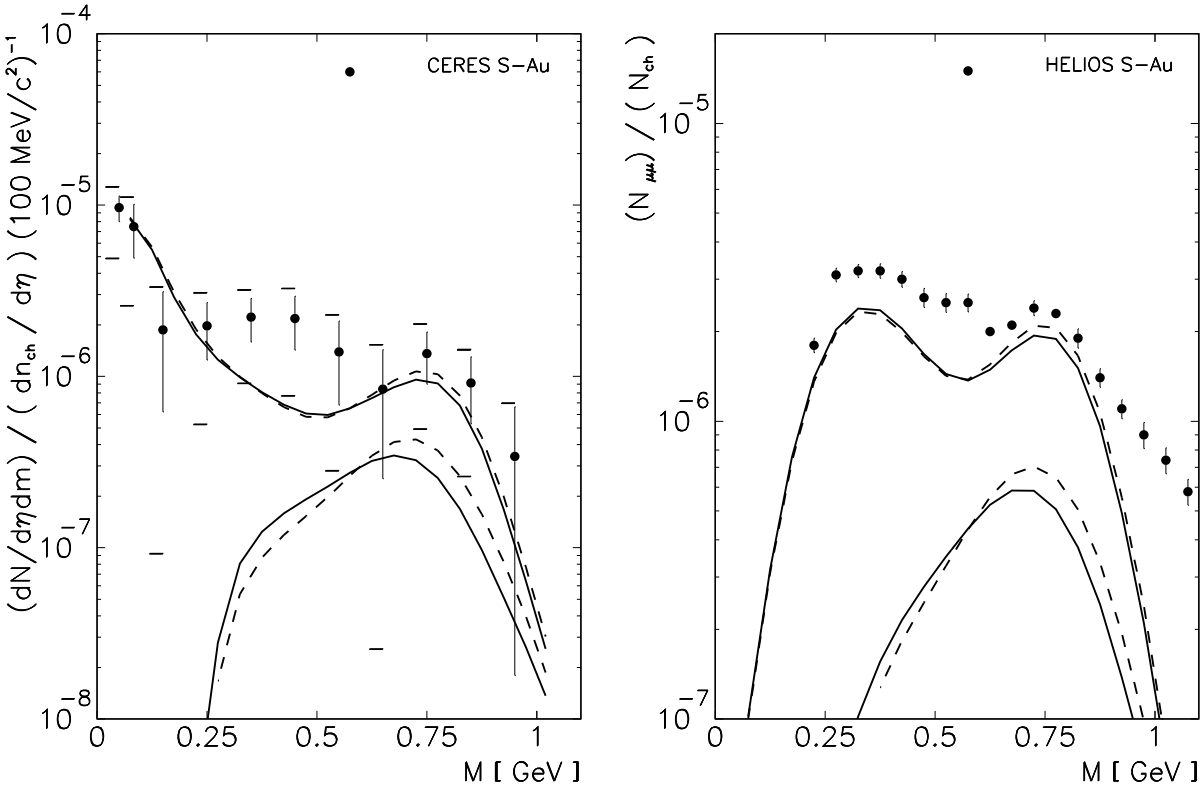


Figure 10: Dilepton production for parameter set 3 with (full lines) and without (dashed lines) in medium modification of the pion annihilation cross section.

Comparing with the changes in the dilepton yield we could generate by altering the initial conditions for the hadronic phase, the effect of the in medium corrections is small. We, therefore, have to conclude that it is probably impossible to learn something about the in medium pion dispersion relation from SPS-energy dilepton experiments unless the dynamics of the hadronic phase is extremely well known, and of course, much more precise measurements are feasible.

6.3 Prediction for Pb+Pb

Currently, the system $Pb+Pb$ at 150 GeV/A is investigated by the CERES collaboration so that it seems useful to try to make some predictions on what we would expect for the dilepton yield of this large system. Within our approach, this can only be a rough estimate, since final hadronic data for this system are not yet available. However, preliminary results for the rapidity distribution of negatively charged particles from the NA49 collaboration [46] as well as preliminary spectra from the NA44 collaboration [42] are available. NA44 reports that the slope parameter for pion transverse momentum spectrum changes only little when going from S+Pb to Pb+Pb. We, therefore, require that the final pion spectrum agrees with the S+Au data from the NA35 collaboration up to an overall constant. Our resulting rapidity distributions are shown in figure 11 together with preliminary data from the NA49 collaboration [46].

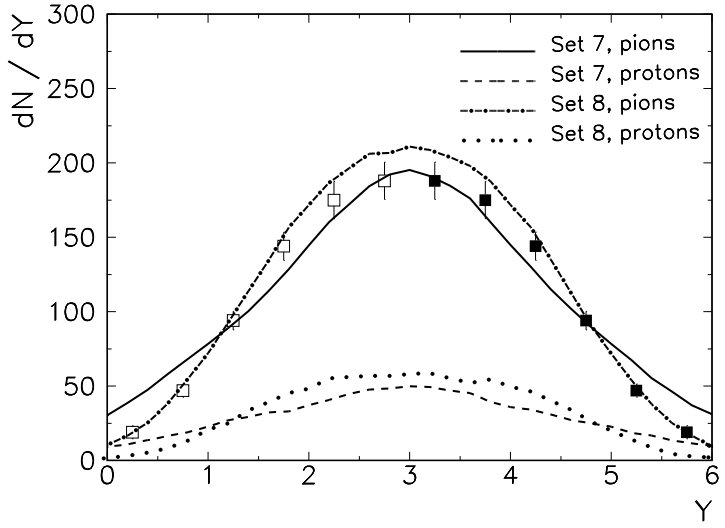


Figure 11: Pion and proton rapidity distribution for Pb+Pb. Data points are preliminary results for negatively charged hadrons from the NA49 collaboration.

In figure 12(a) we show our prediction for the Pb+Pb result, based on the CERES acceptance and normalization, i.e. dileptons per charged particles. The parameterizations we have used are given in table 1 (sets 7 and 8). They follow the same philosophy as sets 3 and 5 for the S+Au case, respectively. In order to model a hadronic system generated in Pb+Pb collisions we increased the transverse radius to 6.5 fm and the number of total pions (~ 2000) and baryons (400). The relative abundances are the same as in sets 3 and 5, respectively.

For a comparison, we also show the results for S+Au obtained with parameter set 3. We find, that if normalized to the number of charged particles, the dilepton spectrum hardly changes by going from S+Au to the heavier system of Pb+Pb. This result may be surprising at first sight, because in the heavier system many more pions are created which should give rise to more dileptons from pion annihilation. However, one has to be a little careful with this argument. The rate of dilepton production from pion annihilation is roughly proportional to the square of the pion *density*

$$\frac{dN_{e^+e^-}}{V\tau} \sim \rho_\pi^2 \tag{22}$$

where V is the the volume and τ is the lifetime of the fireball and ρ_π the average pion density. Consequently, the total number of dileptons produced divided by the number of charged particles (mostly pions) is *linearly* proportional the average pion density

$$\frac{N_{e^+e^-}}{N_{charged}} \sim \frac{\tau V \rho_\pi^2}{N_{charged}} \sim \tau \rho_\pi \tag{23}$$

Here we assumed that $N_{charged} \sim N_\pi$. It is probably fair to assume that the volume of the fireball scales like the volume of the initial nuclei and, therefore, more or less like A, the number of nucleons. But also the number of produced pions (negatively charged hadrons) seems to scale the same way. NA35 reports about 100 negative pion produced in S+S collisions [47] and NA49 a preliminary number of about 700 in Pb+Pb collisions [46]. Consequently, since both the volume and the number of pions seem to scale more or less with the size of the system, the average pion density reached in these collisions is essentially independent of the system size. Remains the lifetime of the fireball, τ, which is probably larger for a bigger system but depends on the detailed expansion dynamics. The effect of the lifetime is demonstrated in figure 12(b), where the contributions of the pion annihilation is plotted. If we compare the results for S+Au (set 5) with those for Pb+Pb (set 8), we find about a factor of 2 increase around the ρ-ω mass. In both calculations the initial pion density is roughly the same, so that difference comes from the longer lifetime of the larger system.

Notice, that the CERES experiments accepts dileptons in the rapidity interval $2.1 \leq Y \leq 2.65$ and, thus, favors the S+Au system, which has a fireball rapidity of about $Y = 2.6$, whereas Pb+Pb is located at $Y = 3$. This difference in acceptance is also the reason why the increase in the pion annihilation contribution is not reflected in the total yield, especially around the ρ-ω mass. Dileptons from ω and initial ρ mesons, which scale like the number of charged particles, contribute less.

Again, our proposed in medium modification due to the pion dispersion relation leads only to a small correction (see dotted curve in figure 12(a)).

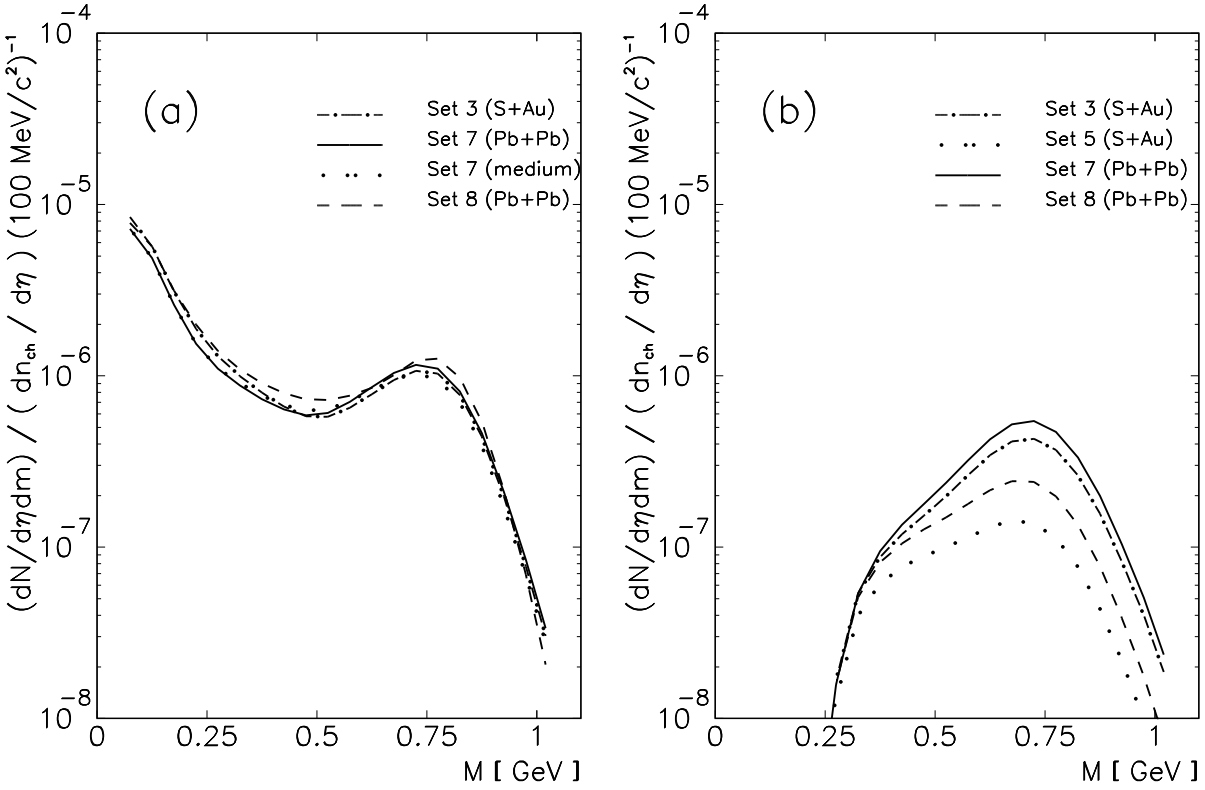


Figure 12: Prediction for Pb+Pb. (a) Total yield, (b) contribution from pion annihilation

To summarize our prediction, if there are no in medium effects such as dropping ρ masses, we expect that the dilepton spectrum for Pb+Pb subject to the CERES acceptance and normalization should not differ significantly from that for S+Au. If the statistical and systematic errors are smaller for the Pb+Pb data, as expected [48], we would actually expect that in the mass region of $400 - 500$ MeV the central values should come down somewhat as compared to the published S+Au data. If, on the other hand, the Pb+Pb data show a significant increase over S+Au, some additional, prehadronic production mechanism or strong in medium modifications such as dropping vector meson masses etc. would be called for.

6.4 Baryon decays

In our calculation we have not taken into account the possible Dalitz decays of any baryons. While we have taken into account the Delta resonance for the expansion dynamics we have not included its Dalitz decay mainly because it will only contribute to

invariant masses lower than 300 MeV. However, at the temperatures considered also heavier baryon resonances will be present. For a temperature of 180 MeV we find that about 12 % of the baryon number will be in states heavier than the Roper resonance ($N^*(1440)$), such as the $N^*(1520)$, $N^*(1535)$, the $\Delta(1600)$, and the $\Delta(1620)$. While the $N^*(1440)$ hardly couples to photons (the branching ratio is smaller than a tenth of a percent) the higher nucleon and Delta states have considerable photon decay width. Also their masses are large enough such that the Dalitz decays could contribute to the relevant region around 400 MeV. Since the lifetime or these resonances is rather short ($\Gamma \geq 150$ MeV) the dominant contribution to the dilepton spectrum will come during the lifetime τ of the fireball, where we may assume a constant number of these resonances. The total contribution to the dilepton yield, therefore, is

$$N_{e+e-}^{baryons} = \tau N_{baryons} \Gamma_{e^+e^-}^{baryons} + N_{baryons} \frac{\Gamma_{e^+e^-}^{baryons}}{\Gamma_{tot}^{baryons}} \tag{24}$$

The second term takes into account the contribution after freeze. It can be ignored for our estimate since the lifetime of the resonances $1/\Gamma_{tot}^{baryons}$ is much smaller that that of the fireball (τ).

To give an upper limit for the contribution we assume a lifetime of $\tau = 10$ fm/c for the fireball and that the heavy baryons constitute 25 % of the total baryon number (which is a factor of *two* more than chemical equilibrium would suggest at a temperature of 180 MeV). For the Dalitz decay width $\Gamma_{e^+e^-}^{baryons}$ we use the formula (4.8) of Wolf et al. [41], which has been derived for the Dalitz decay of the Delta of a given mass M. The coupling we adjust by assuming that the partial width into photon plus nucleon is 1 MeV, which again is on the large side. For the mass we chose $M = 1.6$ GeV which is in between the nucleon and Delta excited states under consideration. Finally, as done in all calculations, we assume that there are 60 baryons in the fireball, so that we are dealing with 15 high mass baryons.

As a reference we use the Dalitz decay of the ω meson, since its contribution can also be simply estimated. Due to its small decay width, most ω mesons decay after freeze out and, therefore, their contribution is given by

$$N_{e+e-}^{\omega} = N_{\omega} \frac{\Gamma_{e^+e^-}^{\omega}}{\Gamma_{tot}^{\omega}} \tag{25}$$

In fig. (13) we show the ratio between Dalitz decays from the baryon and that of the ω mesons, assuming that there are 24 ω mesons at freeze out. This number is comparable with our calculation presented in fig (3). We see that even with our optimistic assumption the contribution of the baryons to the dilepton spectrum is less the half of that from the Dalitz decay of the ω. It is probably fair to assume that the experimental acceptance cuts

apply equally to both. By comparing with the result shown in fig. (3) we thus conclude that the contribution of the baryon Dalitz decays only lead to a small correction $\simeq 10\%$ to the results presented above, which may be slightly larger but certainly not significant in case of Pb+Pb.

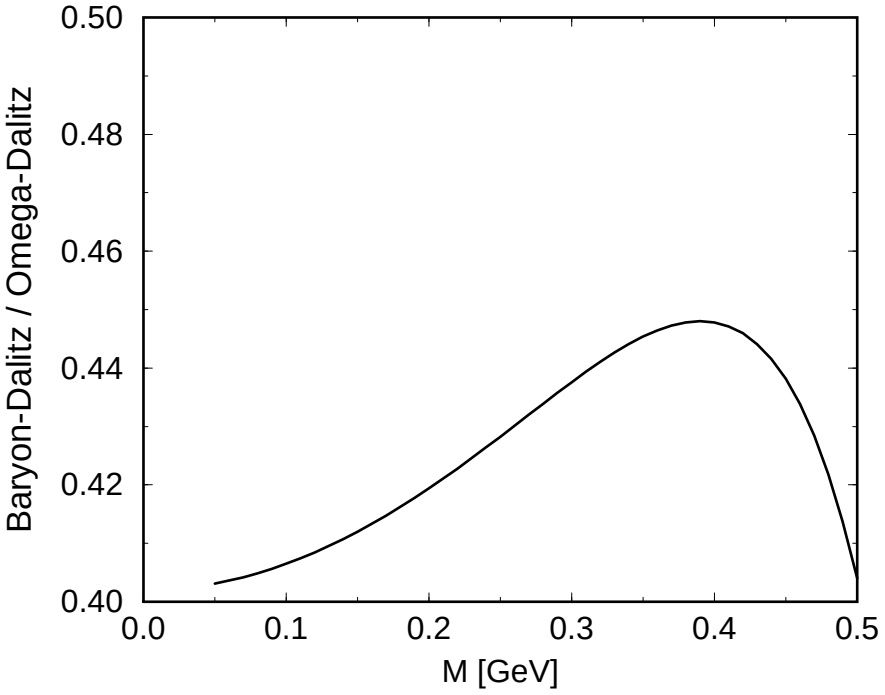


Figure 13: Ratio of baryon-Dalitz decay over ω-Dalitz decay

7 Conclusion

In this article we have studied dilepton production form a hadronic system believed to be created in an SPS energy heavy ion collisions. We have addressed the question to which extent dilepton data provide information on the equilibration dynamics in the hadronic phase. To this end we have investigated several different initial conditions for the hadronic phase, subject to the constraint that the final hadronic observable agree with the data. The comparison with the dilepton data could rule out an initial state where the relative abundances of hadrons is given by chemical equilibrium based on a large pion chemical potential. Variations of the initial momentum and configuration space

distributions affected the dilepton invariant mass spectrum by not more than a factor of two, which is small compared to the error bars of the data. Therefore, with the presently available data, the question of the equilibration dynamics can not be settled.

We were not able to find a scenario which would give enough dilepton in the mass region around $400 - 500\,\mathrm{MeV}$ to reach the central values of the CERES data. Our 'best' results agrees with the lower end of the sum of statistical and systematic errors in the region. Considering the large experimental uncertainties we can not conclude that any in medium modifications are needed in order to explain the present data.

We predict essentially the same dilepton spectrum for the larger system Pb+Pb as for S+Au, provided the CERES acceptance and normalization are used. Since for this system smaller experimental errors are expected, these data may give very valuable information about possible in medium corrections such as dropping vector meson masses.

We have investigated the effect of an in medium pion dispersion relation and pion form factor on the dilepton spectrum. While the effect is visible in the pion annihilation channel, it hardly affects the total dilepton yield. Therefore, unfortunately it seems rather unlikely that the presence of an in medium pion dispersion relation can be detected in SPS-energy heavy ion collisions.

Our conclusions could be much more sharpened if precise measurements of the the η mesons and the ω mesons would be available. The latter, of course, could be obtained best with a considerably improved mass resolution of the dilepton spectrometer. However, a careful measurement of the transverse momentum spectrum in the ρ - ω mass region would already provide some information on the relative importance of the omega decays. Further constraints could be obtained by looking at pion correlation (HBT) data. These may provide valuable information about the space-momentum correlations and thus restrict our choices of initial conditions. However, considering, the rather weak sensitivity of the dilepton data with respect to the variation of the initial phase space, we do not expect much additional insight from such an investigation.

Acknowledgements: We would like to thank the CERES collaboration, in particluar A. Drees, I. Tserruya and Th. Ullrich for many useful discussions concerning their data. We would further like to thank the NA35 collaboration and in particular G. Odyniec for providing the data files for the hadronic spectra. V.K. would especially like to thank G.Q. Li for aggreeing to and helping in a detailed comparison of our transport models. Helpful discussions with G.E. Brown and C.M. Ko are also acknowledged.

References

[1] P.V. Ruskanen, Nucl. Phys. **A544** 169c (1995).

[2] V. Koch, Proceedings of Workshop on *'Soft Lepton Pair and Photon Production'*, Pittsburgh, 1990, Nova Science Publishers (1992).

[3] Gy. Wolf, W. Cassing, and U. Mosel, Nucl. Phys. **A552** 549 (1993).

[4] C. Song, S.H. Lee, and C.M. Ko, Phys. Rev. **C52** R476 (1995).

[5] C. Song, V. Koch, S.H. Lee, and C.M. Ko, Phys. Lett. **B52** 379 (1996).

[6] C. Song and V. Koch, LBL-Report 38362, to be submitted to Phys. Rev. C.

[7] G.Q. Li and C.M. Ko, Nucl. Phys. **A582** 731 (1995).

[8] H.S. Matis, Nucl. Phys. **A583** 617 (1995).

[9] G. Agakichiev et al., Phys. Rev. Lett. **75** 1272 (1995); J.P. Wurm for the CERES/NA45 collaboration, Nucl. Phys. **A590** 103c (1995); A. Drees for the CERES/NA45 collaboration' *Proc. International Workshop XXIII on Gross Properties of Nuclei and Nuclear Excitations*, ed. H. Feldmeier and W. Nörenberg, (GSI, Darmstadt 1995) p. 151.

[10] M. Masera for the HELIOS-3 Collaboration, Nucl. Phys. **A590** 93c (1995); I. Kralik for the HELIOS-3 Collaboration, *Proc. International Workshop XXIII on Gross Properties of Nuclei and Nuclear Excitations*, ed. H. Feldmeier and W. Nörenberg, (GSI, Darmstadt 1995) p. 143.

[11] G.Q. Li, C.M. Ko, and G.E. Brown, Phys. Rev. Lett. **75** 4007 (1995); Nucl. Phys. **A**, in print.

[12] W. Cassing, W. Ehehalt, and C.M. Ko, Phys. Lett. **B363** 35 (1995).

[13] D.K. Shrivastava, B. Sinha and C. Gale, Phys. Rev. **C53** 567 (1996)

[14] K. Haglin, MSU-preprint MSUCL-978, nucl-th/9604035 (1996)

[15] R. Pisarski, Phys. Lett. **B110** 155 (1982).

[16] G.E. Brown and M. Rho, Phys. Rev. Lett **66** 2720 (1991).

[17] C. Gale and J. Kapusta, Phys. Rev. **C35** 2107 (1987).

[18] C.L. Korpa and S. Pratt, Phys. Rev. Lett. **64** 1502 (1990).

[19] C.L. Korpa, L. Xiong, C.M. Ko, and P.J. Siemens, Phys. Rev. Lett. **B246** 333 (1990).

[20] E.V. Shuryak, Nucl. Phys. **A533** 761 (1991).

[21] C. Song, Phys. Rev. **D49** 1556 (1994).

[22] R. Rapp, G. Chanfray, and J. Wambach, Phys. Rev. Lett. **76** 368 (1996).

[23] P. Braun-Munzinger, J. Stachel, J.P. Wessels, and N. Xu Phys.Lett. **B365** 1 (1996).

[24] P. Braun-Munzinger, J. Stachel, J.P. Wessels, and N. Xu Phys.Lett. **B344** 43 (1995).

[25] H. Sorge, H. Stöcker, and W. Greiner, Ann. Phys. **192** 266 (1989).

[26] K. Werner, Phys. Rept. **232** 87 (1993).

[27] R. Santo et al., Nucl. Phys. **A566** 61 (1994).

[28] B. Blättel, V, Koch, and U. Mosel Rep. Prog. Phys. **56** 1 (1993).

[29] P. Danielewicz and G. Bertsch Nucl. Phys. **A 553** 712 (1991).

[30] G.F. Bertsch and S. DasGupta Phys. Rep. **160** 189 (1988).

[31] R.K. Badhuri, Models of the Nucleon, (Addison-Wesley, Reading, MA, 1988).

[32] L. Xiong, E. Shuryak, and G.E. Brown, Phys. Rev. **D46** 3798 (1992).

[33] C. Song Phys. Rev. **C47** 2861 (1993).

[34] NA35 preprint IKF-HENPG 6-94

[35] E. Schnedermann, J. Sollfrank, and U. Heinz, Phys. Rev. **C48** 2462 (1993).

[36] L.G. Landsberg Phys. Rept. **128** 301 (1985).

[37] M. Dey, V.L. Eletzky, and B.L. Ioffe, Phys. Lett. **252B** 620 (1990).

[38] C. Song, Phys. Rev. **D48** 1375 (1993).

[39] R.D. Pisarski, Phys. Rev. **D52** 4694 (1994).

[40] V.Koch and G.F. Bertsch, Nucl. Phys. **A552** 591 (1993).

[41] Gy. Wolf et al., Nucl. Phys. **A517** 615 (1990).

[42] J. Dodd for the NA44 collaboration, Nucl. Phys. bf A590 523c (1995).

[43] Thomas Ullrich, private communication.

[44] S.H. Lee, C. Song, and H. Yabu, Phys. Lett. **B341** (95) 407.

[45] K. Haglin, Nucl. Phys. **A584** 719 (1995)

[46] R. Stock, *Proceedings to the Internation Conference on Nuclear Physics, Bejing, China, 1995*

[47] D. Röhrich for the NA35 collaboration, Nucl. Phys. **A566** 35c (1994)

[48] I. Tserruya, private communication.